

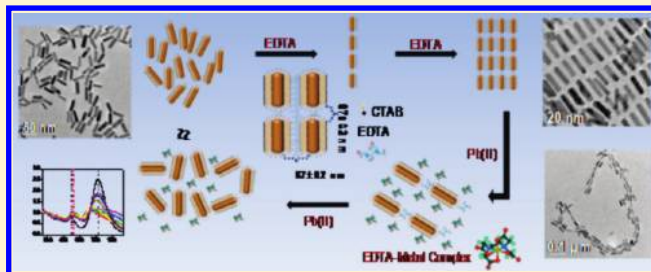
Reversible Assembly and Disassembly of Gold Nanorods Induced by EDTA and Its Application in SERS Tuning

T. S. Sreepasad and T. Pradeep*

DST Unit of Nanoscience, Department of Chemistry, Indian Institute of Technology Madras, Chennai-600 036, India

Supporting Information

ABSTRACT: A facile and reversible method for assembling and disassembling gold nanorods (GNRs) using a common chelating agent, ethylenediaminetetraacetic acid (EDTA), is reported. Assembly was induced by the electrostatic interaction between the cetyltrimethylammonium bromide (CTAB) bilayer present on GNRs and EDTA. At lower concentrations of EDTA, end-to-end assembled chains were formed. At higher concentrations of EDTA, these chains come together to form sheet-like structures. The complex of CTAB and EDTA, being labile, disassembles in the presence of stronger chelating agents. Upon addition of metal ions having higher formation constants, EDTA detaches from the GNRs and forms stronger complexes with metal ions, resulting in disassembly. Characteristic changes were observed in the UV/vis spectra. Addition of EDTA resulted in a red shift of longitudinal surface plasmon (LSP) resonance at lower concentrations, indicating an end-to-end assembly. At higher concentrations, the characteristic of side-by-side assembly was seen in the UV/vis spectra. TEM analysis proved the existence of end-to-end chains at lower concentrations of EDTA and side-by-side assembled sheet-like structures at higher concentrations. The addition of metal ions induced disassembly. Even 2 ppb of metal ion was detected using the spectral changes. Disassembly was studied in detail, taking Pb(II) as the model system. Upon addition of Pb(II), TSP showed a blue shift and decreased in intensity while the LSP showed a red shift and increased in intensity. A new peak at a higher wavelength region emerged, pointing to the existence of both side-by-side and end-to-end assembly in the system. TEM analysis showed that the disassembly involves the formation of bundled chains which may be the reason for the observed spectral changes. Surface-enhanced Raman scattering (SERS) activity of the system could be tuned by controlling the concentration of EDTA and the metal ion, Pb(II).



INTRODUCTION

Gold nanorods (GNRs) belong to one of the most studied classes of anisotropic nanosystems.¹ Because of their size-dependent photophysical properties, they are useful for diverse processes.¹ The characteristic absorption maxima of gold nanorods can be precisely tuned in the visible to near-infrared region by controlling the aspect ratio. This can be done either during or post synthesis^{1e,2} by appropriate chemistry. Even though the individual nanoparticles themselves are interesting for studying the properties, the assembled macrostructures of these nanoparticles are more readily employed in technologies.³ Such structures have collective properties that result from the coupling of the optical and electronic properties between the interacting particles. Self-assembly of GNRs into one-, two-, or even three-dimensional (3D) functional superstructures is attracting a lot of interest. They are known to self-assemble on carbon grids upon solvent evaporation, through the interaction between cetyltrimethylammonium bromide (CTAB) bilayers on the surface.⁴ This kind of self-assembly is very difficult to control, and obtaining the desired assembled structure and corresponding property is very tedious.⁴ “Programmed self-assembly”, where the self-assembly is aided by the addition of external molecules, is the most explored technique to create assembled structures.⁵

The inherent anisotropic shape of gold nanorods allows them to assemble in different ways, namely, in an end-to-end or side-by-side manner. Depending on the type of assembly, the optical properties vary.⁶ Several strategies such as electrostatic interactions,⁷ hydrogen bonding,⁸ covalent bonding,⁹ van der Waals and dipole interaction,¹⁰ antibody/antigen or DNA-based biorecognitions,¹¹ using templates such as carbon nanotubes,^{12a} water droplets,^{12b} microgels,^{12c} and silica microspheres,^{12d,e} and interactions between functionalized polymers in selective solvents known as polymer tethering¹³ have been employed to assemble GNRs.

The ability of acids to assemble GNRs into well-ordered superstructures has already been reported.^{7b,c} At a particular concentration of gold nanorods and acids, when the pH is adjusted to an optimum value, acids can neutralize the electrostatic repulsion between GNRs sufficiently so that the NRs can come together to form superstructures. Various examples of this kind of assembly exist in the literature.^{7b,c} We have recently reported a versatile assembly of GNRs induced by DMSA.

Received: December 4, 2010

Revised: February 5, 2011

Published: March 02, 2011

Depending upon the concentration of DMSA present, GNRs can be assembled into 1-, 2-, and 3-D superstructures where NRs can exist either parallel or perpendicular to the surface.^{7b}

Organization of nanomaterials has seen significant progress, but disassembling these assembled superstructures is often difficult and has been met with only limited progress. In all examples mentioned above, once the assembly is formed in solution, further manipulation of it was not possible. The nature of the assembly remained the same once the structure was formed. Changing the nature of the assembly or ultimately disassembling the superstructures was always a problem in electrostatically assembled superstructures^{14,15} Thiol-modified DNA oligomers were utilized for the reversible aggregation of spherical gold nanoparticles.¹⁴ Wang et al. recently reported a versatile method for the reversible assembly and disassembly of GNRs.^{15a} End or side surfaces of GNRs were functionalized selectively by thiol-containing bifunctional molecules such as 3-mercaptopropionic acid (MPA), 11-mercaptopundecanoic acid (MUA), glutathione (GSH), and cysteine (CYS).^{15a} Depending upon the pH of the solution, these molecules either induce the assembly of Au nanorods or disassemble them. This reversible, pH-controlled assembly and disassembly was found to be repeatable several times. Newkome et al. devised a method for the end-to-end assembly and disassembly of GNRs through a custom-made complex.^{15b} They synthesized [(disulfide-terminated tpy)₂-M^{II}] and found that GNRs assemble through bis(terpyridine)–metal connectivity, and that facile disassembly occurred upon treatment with aqueous NaOH for the Fe(II) linker and upon treatment with excess Cd(NO₃)₂·4H₂O for the Cd(II) linker.^{15b} The aforementioned reports suggest facile assembly and disassembly, but the nature of the assembly, once formed, remained the same until it was disassembled into individual rods. Manipulating the assembly in such a way that a side-by-side assembly changes to an end-to-end assembly and vice versa has not been achieved. Here, a simple strategy for the assembly and disassembly of GNRs by using ethylenediaminetetraacetic acid (EDTA) is reported. The disassembly process was induced by the addition of metal ions, and even very low concentrations of metal ions (in the range of ppb) can be detected in this process. The addition of EDTA into the GNR solution resulted in the side-by-side assembly of gold nanorods. When metal ions are added into this mixture, the characteristics of the assembly changed. As the concentration of metal ion added increased, the side-by-side assembly changed into an end-to-end assembly, and at a particular concentration of metal ion, the assembly is completely disrupted into individual nanorods. This process was not specific to any metal ion; thus, the system can act as a universal metal ion detector. The mechanism of the assembly and disassembly was investigated, taking Pb(II) as the model system. SERS activity of the structures formed was investigated and found that it can be tuned by controlling the concentration of EDTA and the metal ion. The process was reversible up to three times, and subsequently the NRs underwent irreversible aggregation and settled.

MATERIALS AND METHODS

Sodium borohydride (NaBH₄) was purchased from Sigma-Aldrich. Tetrachloroauric acid trihydrate (HAuCl₄·3H₂O) and silver nitrate (AgNO₃) were purchased from CDH, India. Ascorbic acid was purchased from Himedia Chemicals, India. CTAB and EDTA were purchased from SD Fine Chemicals. Acetates of Pb, Mn, Cu, Zn, Cd, and Hg (all in divalent state) were purchased from Merck. Iron(II) chloride tetrahydrate was purchased from Aldrich. FeCl₃ was purchased

from Himedia Laboratories Pvt. Limited. All chemicals were used as received without further purification. Triply distilled water was used throughout the experiments.

Synthesis of Gold Nanorods. Nanorods were made using the well-established seed-mediated method^{1d} and purified as per the procedure described in our previous paper.^{2b} Briefly, gold seeds (Au@CTAB) of around 3–4 nm diameter were prepared by the NaBH₄ reduction method in the presence of CTAB. Seeds were incubated for 3 h, and then a calculated amount of them was added to a previously prepared growth solution containing specific amounts of CTAB, HAuCl₄, and ascorbic acid. This mixture was kept undisturbed for 24 h and then examined using TEM.

The pristine nanorod sample was centrifuged at 11 000 rpm for 15 min. The supernatant was discarded, and the residue was redispersed in an equal amount of triply distilled water. This process was repeated twice to remove the excess surfactant and other residual reactants. The centrifuged samples were diluted to an optical density of 2.5 at 760 nm (LSP), and the GNR concentration was maintained constant in different samples.

Assembly and Disassembly of Nanorods. The assembly process was initiated by the addition of EDTA to the purified GNRs. For this, calculated amounts of EDTA were added to 4 mL of the purified GNR solution so that the required final concentrations of EDTA were in the range 0.1–1 mM. At higher concentrations, an immediate color change was observed, from brown to violet, indicating assembly-induced aggregation. For disassembly, different metal ions at various concentrations were added to this mixture, and the spectral changes were analyzed by UV/vis spectroscopy (Perkin-Elmer Lambda 25). Aliquots of some samples were drop-casted on carbon-coated copper grids and analyzed with TEM (JEOL 3011, 300 kV TEM with a UHR polepiece).

RESULTS AND DISCUSSION

GNRs are known to show two maxima in the UV/vis spectrum.¹ The first one is due to the plasmon excitation along the long axis, occurring in the NIR region, and is called the longitudinal surface plasmon (LSP) resonance, which will change position according to the length of the nanorod.² The second is due to an excitation along the short axis, occurring in the visible region around 510 nm, called the transverse surface plasmon (TSP) resonance and also gives an indication about the amount of spherical particles in the ensemble, whose feature appears at 520 nm.² The UV/vis spectrum of the purified nanorods after the centrifugation–redispersion cycle is shown in Supporting Information Figure S1A. For a particular synthesis, the LSP was centered at 765 nm and TSP was at 511 nm. The latter showed a small hump around 520 nm pointing to a small amount of spherical nanoparticles which are the byproduct of the synthesis and are difficult to avoid completely. However, the asymmetry was not significant and the LSP was very sharp in nature, indicating the monodispersity of the formed nanorods. Only very few spherical nanoparticles were present. The inset of Figure S1A shows a large area TEM image of this purified sample. GNRs were distributed isotropically without any preferential ordering in most parts of the grid. They had a length of $\sim 35 \pm 4$ nm and breadth of $\sim 11 \pm 3$ nm. Figure S1B shows a high magnification image of the tip of a nanorod. We can clearly see the nanorod crystal structure, devoid of any defects. It is well established that the tips of the nanorods are composed of {111} and {100} facets and the rod body is primarily composed of {110} facets (Figure S1B).¹⁶ Recent investigations suggested that high index planes such as {250} are present on the tips of the nanorods.^{16b}

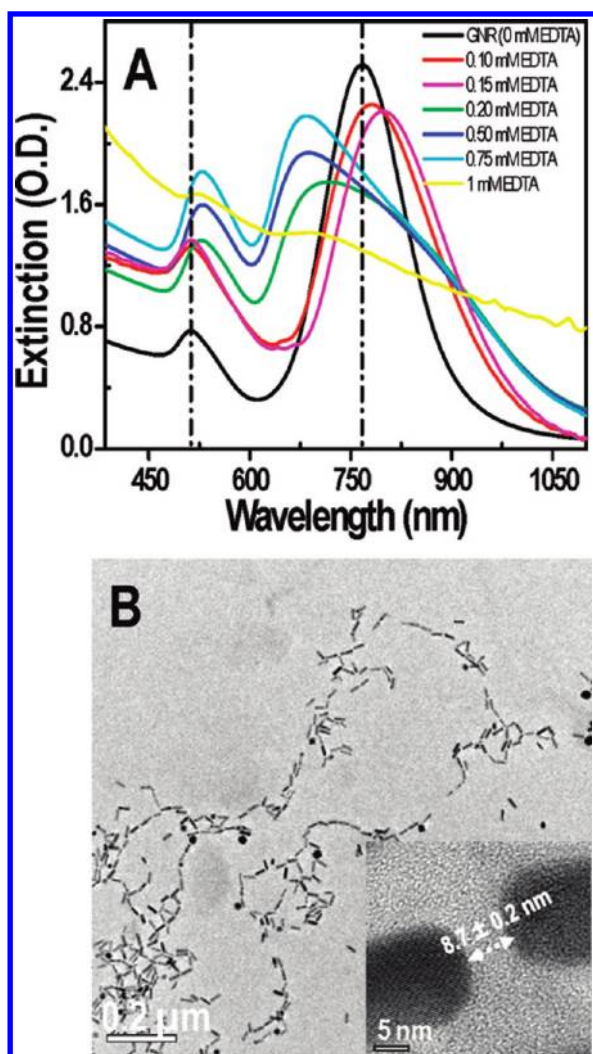


Figure 1. (A) UV/vis spectra showing the effect of addition of EDTA into the GNR dispersion. (B) Large area TEM image of chains formed at 0.15 mM concentration of EDTA. The inset shows the lattice-resolved image of the tips of NRs arranged in an end-to-end fashion.

Formation of Assembled Structures. The surface of the NRs is positively charged because of the presence of a CTAB bilayer.^{2b} Upon neutralization of these charges, the nanorods can be arranged.^{7b,c} We used EDTA, which in the ionized state can neutralize the charge and thereby assemble GNRs. The effect of addition of different concentrations of EDTA into GNRs is shown in Figure 1A. At a lower concentration of EDTA (0.10 mM and 0.15 mM), the LSP showed a slight red shift. The TSP remained unchanged in position but increased in intensity. These spectral changes point to a chain-like arrangement of GNRs where they are arranged in an end-to-end manner. End-to-end assembly of nanorods is known to produce a red shift for the LSP due to interplasmon coupling between the constituent nanorods.⁶ Acids in the anionic form are reported to induce long chains where nanorods are arranged in an end-to-end fashion.¹⁷ GNR samples were centrifuged three times. Hence, a large fraction of CTAB on the end faces will be displaced, and end faces will be available to a greater extent. Hence, an incoming molecule will feel comparatively less steric hindrance from the end faces compared to the side faces. This might be the reason for preferential interaction with the end faces. However, as the

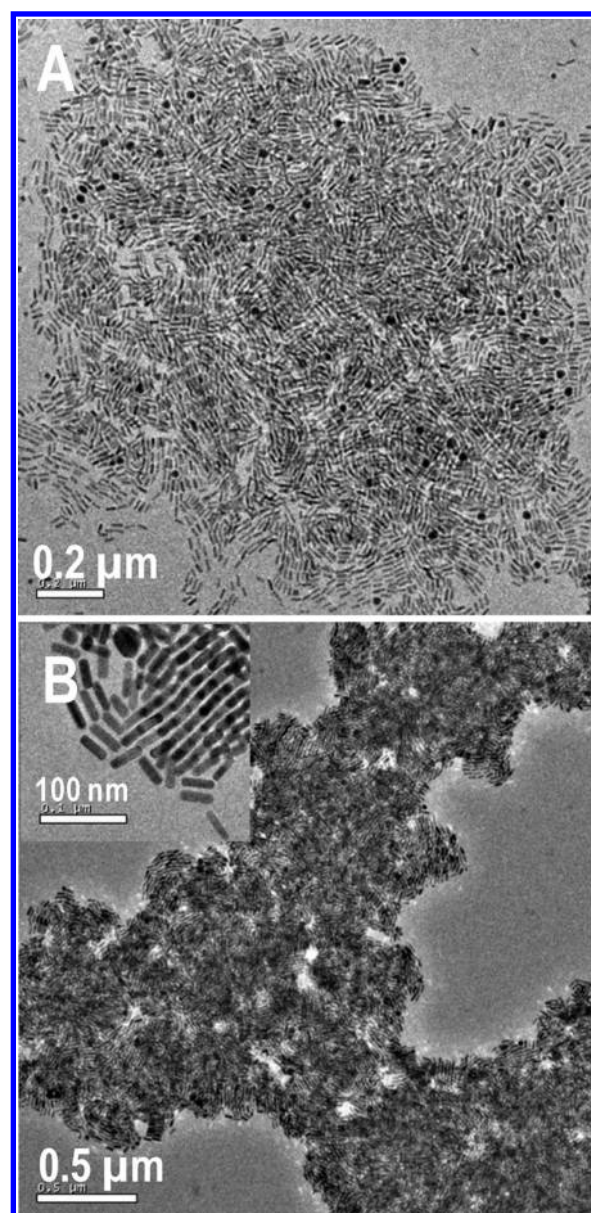


Figure 2. Side-by-side assembled NRs at (A) 0.5 mM EDTA and (B) 1 mM EDTA.

concentration of EDTA increased, all these spectral features changed. At an EDTA concentration of 0.20 mM, the LSP blue-shifted and the TSP shifted to a higher wavelength with an increase in intensity. As the concentration of EDTA increased further, the blue shift in the LSP also increased. Both the shift in the TSP and increase in intensity continued as the concentration of EDTA increased. The blue shift in the LSP and the concurrent red shift in the TSP as well as increase in intensity are reported to be due to the side-by-side assembly of GNRs.⁶ The strength of the LSP coupling is reported to increase with increasing aspect ratio because of the increasing dipole moment of the longitudinal plasmon, both in the case of end-to-end and side-by-side assembly.⁶ This side-by-side assembly can be due to the electrostatic neutralization of the positively charged CTAB bilayer on the side faces of GNRs by ionized EDTA. Similar electrostatic neutralization and formation of the side-by-side assembly are reported earlier.^{7b} Hence, EDTA at lower concentrations tends

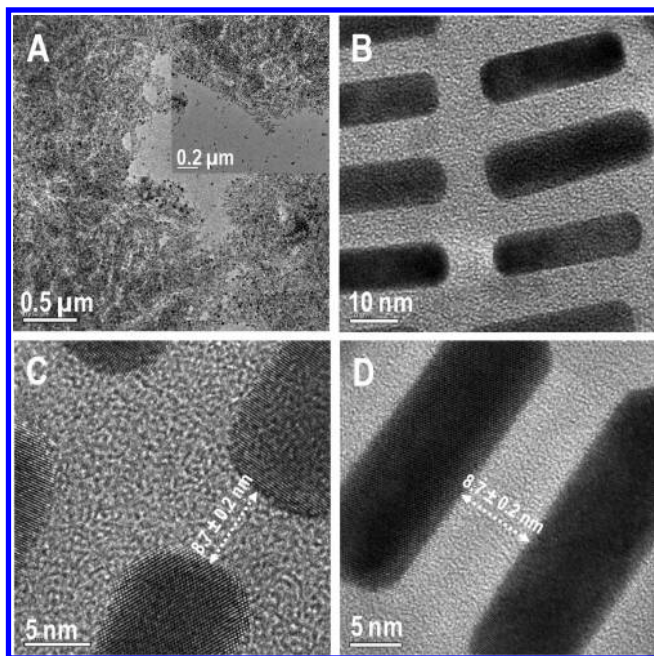


Figure 3. (A) TEM images of a large side-by-side assembled GNR island formed at an EDTA concentration of 0.75 mM. The inset shows a closer view of the edge of an island. (B) Higher magnification image of the same island showing side-by-side assembled NRs. (C) Lattice-resolved TEM image of NRs showing the tip-to-tip arrangement inside the island that also shows spacing between the tips. (D) Lattice-resolved image of side-by-side assembled GNRs showing the spacing between the side faces.

to induce end-to-end assembly and at higher concentrations produces side-by-side assembly.

Figure 1B shows the large area TEM images of the chain-like structures formed from NRs where they are arranged in an end-to-end manner. The inset of Figure 1B shows the lattice-resolved image of the tips of two NRs, arranged in end-to-end fashion. The distance between the tips of two NRs was ~ 8.7 nm. It was reported that acids in the anionic form can arrange NRs end-to-end to form a chain and, that at lower concentrations, these acids in the anionic form are adsorbed only on the end faces of GNRs and will neutralize the surface charge of the GNR at the tips, facilitating the end-to-end assembly.¹⁷ EDTA having four such acid groups is expected to do the same. The sample was purified by centrifugation several times; hence, in some nanorods, the CTAB layer at the end faces can be absent. EDTA can be adsorbed directly on these faces and can facilitate an end-to-end assembly. In this case, the distance between NRs will be much less (~ 1 nm). Similar conclusions can be made for other places in the chains (Supporting Information Figure S2). Upon an increase in the concentration of EDTA, it will get adsorbed on the side faces also. The adsorption of EDTA on the side faces will initiate the interaction of GNRs in a side-by-side manner. So the nature of the assembly changes when the concentration of EDTA is increased, as illustrated by the UV/vis spectra in Figure 1A. The assembly changed from end-to-end to side-by-side.

At higher concentrations of EDTA, NRs started to form islands in which the nanorods are arranged side-by-side. Small islands of GNRs formed as the concentration reached 0.2 mM of EDTA (Supporting Information Figure S3). The end-to-end assembled nanorods, upon neutralization of charges on the side faces, come together and form islands. Further neutralization

may result in a higher extent of side-by-side interaction, causing the changes as indicated in the UV/vis spectra. As the concentration of EDTA increased, increasing amounts of GNRs become assembled and islands grow in size. Figure 2A shows a typical island formed when 0.5 mM EDTA was present in the NR dispersion. The arrangement resembled a collection of GNR chains coming together to form the island. As the concentration is increased further, even multilayers started to form. At an EDTA concentration of 1 mM, GNRs aggregated and started to settle. These aggregates were analyzed with TEM. They also showed side-by-side assembly (Figure 2B). The TEM image taken from an edge of such an assembly (inset in Figure 2B) shows GNRs with a side-by-side stacking, and even the next layer follows a similar stacking.

The side-by-side assembly was investigated in more detail. Figure 3A shows the TEM images taken from the assembly formed at an EDTA concentration of 0.75 mM. We can see an island spread over μm^2 area in which NRs are arranged in a side-by-side fashion. The inset shows a higher magnification image of an edge of one such island. On closer observation, we can see that the nanorod tips are eclipsed to each other (Figure 3B). This points to the argument presented above that end-to-end chains are formed first and that they may be coming together to form the island which will result in an eclipsed conformation of the tips of the nanorod. In an early report, it was found that if the NRs form side-by-side chains first, and then form the sheet-like superstructure, the preferred arrangement would be a staggered arrangement of GNRs.^{7b} However, in most places on the grid, the arrangement was found to be eclipsed. This points to the formation of end-to-end chains first, and further assembly results in the side-by-side assembled superstructure. The formation of standing arrays that fall over the grid can also give rise to a similar configuration.^{4c} However, in the present study, perpendicular arrangement of rods was not seen anywhere on the grid.

The typical distance between the tips was found to be 8.7 ± 0.2 nm. This rules out the possibility of direct attachment of EDTA on the tips. The length of an EDTA molecule has been reported to be 9.1 Å.¹⁸ The direct attachment of EDTA would have resulted in an edge to edge distance of ~ 1 –2 nm (if two EDTA molecules are involved). A larger distance points to the involvement of CTAB in the assembly. GNRs are covered with a bilayer of CTAB, which preserves the rod shape and prevents aggregation. The length of a CTA⁺ is reported to be 2.2 nm.^{7b} The thickness of the bilayer on the nanorod will be smaller than twice the length of CTA⁺, due to interdigitation, and it is calculated to be 3.9 nm.^{7b} So the inter-rod distance is a sum of two bilayers and one EDTA molecule coming together to form the assembly. This is depicted in the scheme presented in Figure 4A. Short-chain diacids having less than six methylene groups are reported to form orthogonal monolayers on metal oxide surfaces with only one terminal acid group interacting with the surface.¹⁹ Adsorption of polyacids on the CTAB-coated nanorod surface is also thought to be similar.^{7b,c} Therefore, we believe that in the assembly, EDTA forms monolayers with a perpendicular orientation on the nanorod surface. In solution, EDTA in the ionized state has negatively charged carboxylate groups that neutralize the CTAB bilayer by the formation of a CTA⁺–EDTA complex²⁰ as shown in the Figure 4A. So the electrostatic neutralization of the bilayer by EDTA brings together NRs, and the intermolecular hydrogen bonding between the EDTA molecules stabilizes the assembly. Electrostatic neutralization of the CTAB bilayer was established by zeta

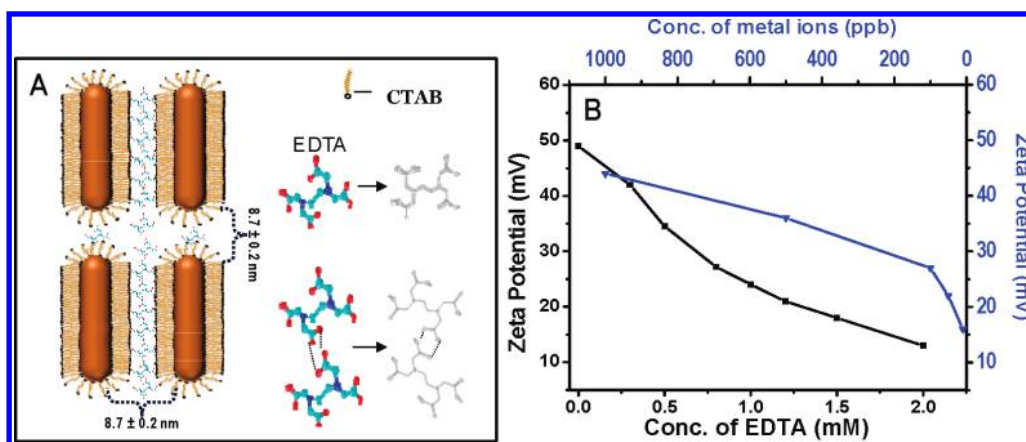


Figure 4. (A) Proposed molecular self-organization leading to the assembly. (B) Change in zeta potential of GNR dispersion upon addition of EDTA (black trace) and the subsequent increase in zeta potential after the addition of metal ion (Pb(II)), indicating the electrostatic nature of the assembly and disassembly (blue trace). EDTA concentration is 0.75 mM.

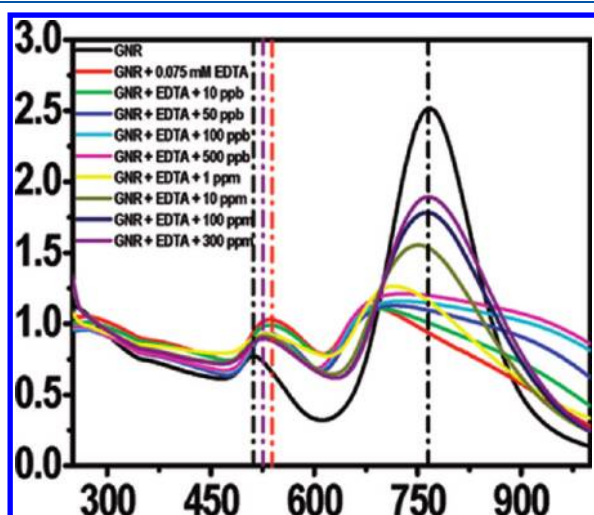


Figure 5. UV/vis spectra showing the spectral changes happening to the side-by-side assembled GNR-EDTA (0.75 mM) sample upon addition of Pb(II).

potential measurements. The data show that upon the addition of EDTA, the zeta potential of GNR dispersion decreases (Figure 4B). The eclipsed conformation between the tips may be facilitating maximum hydrogen bonding between EDTA molecules, which may be the reason for the observed structure of the NR assembly.

Metal Ion-Induced Disassembly. Electrostatic assemblies, once formed, are difficult to disassemble. The rigid nature of the bonding makes it difficult to manipulate the assembly. Changes in the pH can bring about changes in the carboxylic acid functional groups, and this was utilized to bring forth assembly or disassembly.^{15a} However, extreme pH conditions are not favorable for nanorods.^{7b,26} EDTA used in this study is a well-known chelating agent. The formation constants for EDTA with metals are very high, and it forms very stable complexes. The formation constants for ion-pairs such as EDTA-CTAB are comparatively lower^{20a} and therefore labile. Consequently, such an assembly can be easily manipulated by the addition of metal ions. We explored this possibility in detail. EDTA is known to form strong complexes with Pb(II) and Zn(II). Hence, Pb(II) was taken as the model metal ion, and the disassembly

mechanism was studied in detail. Various other species tested are given in the Supporting Information (Figure S4).

Figure 5 illustrates the changes in spectra accompanied by the addition of Pb(II) to EDTA-induced assembly (0.75 mM EDTA). We can see that the LSP starts to red shift and a new peak is becoming evident in the higher wavelength (near IR) region. As the concentration of Pb(II) increases, the LSP shifts increasingly to the higher wavelength region and a new peak emerges in the higher wavelength region. We found that even ppb levels of metal ion can be detected by UV/vis spectral changes (Supporting Information Figure S5). The red shift in the LSP in the side-by-side assembled rods might be due to the disassembly of nanorods while the formation of a small hump in the near IR region indicates the formation of end-to-end assembly.^{6,12a,21} TSP also showed a systematic change. As the metal ion concentration present in the dispersion increased, TSP started to blue shift and decrease in intensity. This also points to the disruption of the side-by-side assembly.⁶ All the above observations point to the change in the nature of GNR assembly induced by EDTA. The side-by-side assembled rods might be changing into end-to-end assembled rods. At a concentration of 1 ppm Pb(II), the LSP is blue-shifted with respect to the initial nanorods and the spectrum has a hump around 950 nm, implying the presence of both side-by-side and end-to-end assembled rods. At a concentration of 200 ppm Pb(II), the LSP almost reaches the initial pristine nanorod position, pointing to the disassembly of GNRs. However, the spectrum had a higher background compared to that of the parent GNR. Also, the LSP was much broader, and the TSP, although blue-shifted, never reached the initial NR position. Further increase in Pb(II) concentration did not change the spectra significantly. All metal ions tested showed similar changes in the UV/vis spectra. Disassembly was manifested in the zeta potential measurement as well. As the concentrations of added Pb(II) increased, the zeta potential of the solution increased. This may be due to the detachment of EDTA from the GNR surface to form stable complexes with Pb(II), thereby increasing the zeta potential (Figure 4B). Anions present in the solution did not show any appreciable effect on disassembly. The EDTA-GNR assembly was investigated in the presence of Pb(CH₃COO)₂ and Pb(NO₃)₂. In both the cases, disassembly occurred (Supporting Information Figure S6), supporting to the argument that anions are irrelevant in the disassembly process.

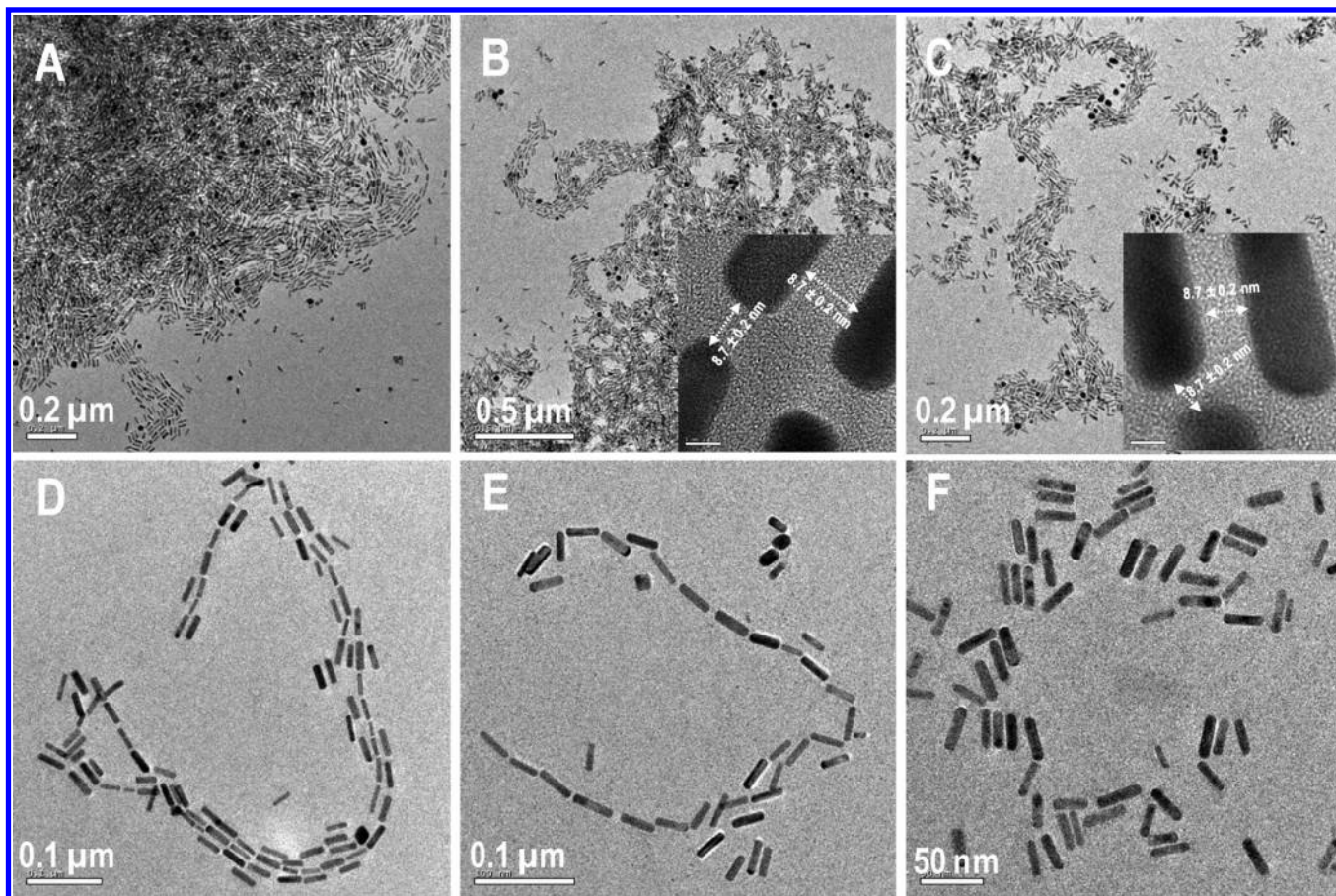


Figure 6. TEM images of EDTA–GNR assembled structures (formed at an EDTA concentration of 0.75 mM) at different Pb(II) concentrations. (A) 0 ppb, (B) 50 ppb, and (C) 500 ppb. Inset figures show the lattice-resolved images of the tips of the nanorods. Linear assemblies formed after the addition of Pb(II): (D) 5 ppm and (E) 25 ppm. (F) Dispersed GNRs without any preferential order at 200 ppm of Pb(II).

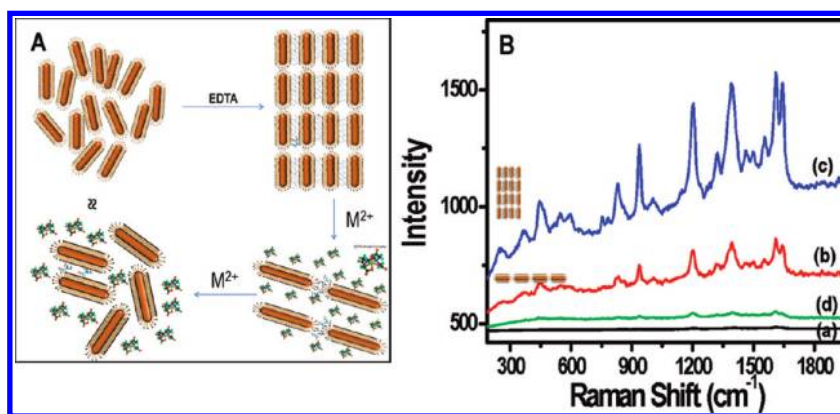


Figure 7. (A) Scheme showing the process of GNR assembly and disassembly. (B) SERS spectra of crystal violet (CV) collected from the GNRs at different assembled states. (a) Parent GNR solution, (b) end-to-end assembled GNRs, (c) fully assembled GNRs, and (d) disassembled GNRs (concentration of CV = 10^{-7} M). The metal ion used is Pb^{2+} .

TEM analysis of the sample at different concentrations of Pb(II) revealed systematic disassembly. At lower concentrations, the side-by-side assembly (formed at an EDTA concentration of 0.75 mM, Figure 6A) changed to bundled chain-like structure (Figure 6B). This could be the reason for the evolution of the new peak at a higher wavelength region. As the concentration of Pb(II) reached 500 ppb, an increasing amount of separated bundles was visible (Figure 6C). In the presence of Pb(II), which

has a higher binding coefficient with EDTA compared to the EDTA–CTAB complex, EDTA is expected to detach from CTAB and form a more stable complex with Pb(II). EDTA bound on the side faces may become detached first and this might give rise to the bundled chains. As an increasing amount of EDTA is detached from the GNRs, individual chains also start to appear (Figure 6D,E). Side-by-side assembled GNRs were always present in the sample. However, the extent of this kind of

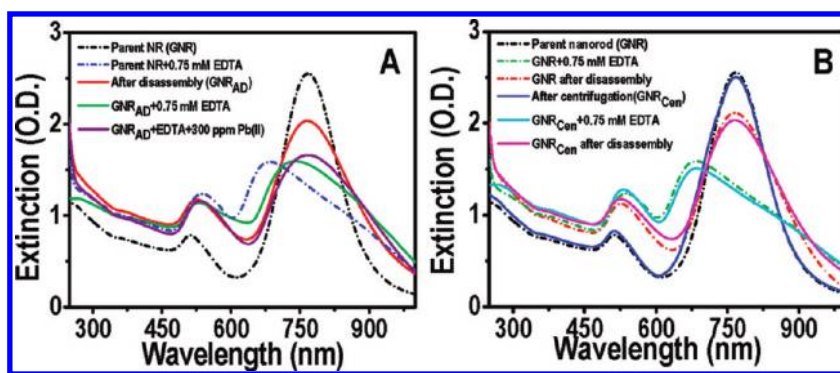


Figure 8. UV/vis spectra of GNR_{AD} upon addition of EDTA (A) without centrifugation and (B) after centrifugation (GNR_{CEN}). The dotted line depicts the spectra of parent nanorods and their assembled structures and disassembly. The solid lines show spectral changes observed when EDTA (0.75 mM) was added to GNR_{AD}, showing the reversible nature of the assembly process.

assembly decreased as the concentration of metal ion added increased. At 200 ppm of Pb(II), most of the assembled nanorods disassembled and the nanorods were distributed on the TEM grids without any preferential order (Figure 6F, Supporting Information Figure S7). In some parts of the grids, small assemblies of nanorods were still seen, but these assemblies were very far from each other and were rare. They were also smaller in dimension compared to the initial assemblies (Supporting Information Figure S8). The presence of these assemblies might be the reason for the broader LSP shown by the disassembled GNRs. The sequence of the reaction is depicted in Figure 7A.

IR spectroscopy was employed to check the validity of the proposed disassembly mechanism (Supporting Information Figure S9). An enlarged view of the spectrum in the range of 1850–1000 cm^{-1} is shown in Figure S9. Initially, EDTA showed prominent peaks at 1710 cm^{-1} (C=O, stretch), 1420 cm^{-1} (OH bend), 1320 cm^{-1} , 1280 cm^{-1} (CO bend), and 1145 cm^{-1} (C–N stretch).²² Initially, gold nanorods had features at 1483 cm^{-1} (δ_a ($\text{N}^+(\text{CH}_3)_3$ of CTAB) and 1370 cm^{-1} (δ_s ($\text{C}(\text{CH}_3)_3$)).²³ The broad feature centered at 1630 cm^{-1} is attributed to H–O–H bending of water. When GNRs and EDTA are mixed, the spectra mostly resembled a superposition of the GNR and EDTA spectra, indicating the presence of both CTAB and EDTA, presumably due to complex formation. The formation of metal complexes is known to show interesting spectral changes in EDTA.²⁴ Pb(II) was added to the GNR–EDTA assembly, and the sample was analyzed by FTIR. Complexation of Pb(II) with EDTA is known to produce an appreciable shift in the peak due to C=O.²⁴ We found that the peak that was centered around 1710 cm^{-1} had shifted to 1743 cm^{-1} , proving the formation of a Pb–EDTA complex that resulted in disassembly.

Effect of pH on Assembly and Disassembly. Assemblies, such as those presented in this report, are known to be affected by changes in pH.^{7,15} We studied the influence of pH on the assembly and disassembly. First, the effect of pH on the assembly formation was investigated. Initially, GNR solutions were neutral (pH \sim 6.8). They were made acidic or alkaline by using HCl or NaOH, respectively. EDTA has four pK_a values, i.e., 2.0, 2.7, 6.2, and 10.0.²⁵ At different pH values, the form of EDTA will be different. At pH = 2, EDTA exists as a neutral form, H_4EDTA . As pH increases, the carboxylic acid groups are ionized sequentially. At pH = 2.7, EDTA exists as H_3EDTA^- (pK_{a2}), at pH = 6.2 as $\text{H}_2\text{EDTA}^{2-}$ (pK_{a3}), and at pH = 10.3 as HEDTA^{3-} (pK_{a4}). Below pH = 1, EDTA exists as H_5EDTA^+ .²⁵ The pH of the initial GNR solution was made less than 2 by the addition of HCl, and

subsequently EDTA was added. At this pH, the nanorods did not show any assembly. Only dispersed GNRs were present on the grid. However, the nanorods were not stable for a long time. After one day, GNRs became settled. The pH of the GNR dispersion was adjusted to 11 by adding NaOH. We found that assemblies are formed at this pH, but no additional stability or ordering was seen. At this pH also, GNRs aggregated after some time. Extreme pH is known to aggregate nanostructures.^{7b,26} When the pH was adjusted to \sim 3.5, small assemblies were found that were predominantly ladder-like (Supporting Information Figure S10). At a pH of \sim 7, well-ordered assemblies were formed. A further increase in pH did not show any appreciable improvement in assembled structures. The GNR suspension was near neutral after two centrifugation–redispersion cycles (pH \sim 6.8). At this pH, EDTA exists as $\text{H}_2\text{EDTA}^{2-}$ and can form the assembled structures that are stabilized through hydrogen bonding.²⁵ Further ionization of carboxylic groups may not have much influence on the assembly. This might be the reason for not observing any improvement of assembly at a higher pH. These observations again emphasized the proposed mechanism.

The effect of pH on the disassembly process was also investigated. After the formation of the GNR–EDTA assembled structures, we changed the pH of the system. The assembled system did not show any appreciable change in the pH range of 6–10. Below pH = 6 there was a broadening of the LSP, and at very low pH (pH < 3) the nanorods became settled. Also at higher pH, the system was found to be unstable and settling was observed. Therefore, it was concluded that a simple change in pH cannot disassemble the system. Control experiments were also performed by adding chelated EDTA to the GNRs. EDTA (0.75 mM) was allowed to complex with Pb(II) (200 ppm). This chelated EDTA–Pb(II) complex was added to the GNR solution. No assembly formation was observed, confirming the above mechanism (Supporting Information Figure S11).

The influence of the oxidation state of metal ion on the disassembly was also tested. The affinity of iron in the Fe(II) and Fe(III) states is found to be different. We tried disassembling the system using GNRs with both of these ions separately. GNRs were found to disassemble with both of these ions. No appreciable changes were observed (Supporting Information Figure S12). This is understandable, since EDTA forms 1:1 complexes with most of the metal ions and the formation constants of both these complexes are many orders of magnitude greater than that of the EDTA–CTAB complex. So in presence of these metals,

EDTA will detach from GNRs and form EDTA–metal ion complexes that result in disassembly.

Tuning of SERS Activity of the Assembled System. Surface-enhanced Raman spectroscopy (SERS) is a potent technique for attaining vibrational information about dilute concentrations of analyte molecules.²⁷ Enhanced Raman signals are obtained when molecules are adsorbed onto roughened surfaces of metals such as silver and gold.²⁷ Anisotropic nanostructures are known to show surface-enhanced Raman scattering (SERS) activity.²⁸ GNRs and their assembled superstructures are known to be highly SERS active.²⁹ We investigated the SERS activity of our GNR assemblies using crystal violet (CV) as the analyte molecule. The Raman spectra of CV adsorbed on the assemblies at different concentrations of EDTA are shown in Figure 7B.

Assembled structures show SERS primarily due to “hot spots”³⁰ formed by the presence of two individual nanoparticles in close proximity. It is known that the electromagnetic field at the hot spots formed between the tips of noble metal nanorods is very high.³⁰ The molecules sitting in close proximity to these sites experience an exceptionally large electromagnetic field, which will enhance the Raman active vibrations of the analyte molecules at these locations. So the change in assembly will result in changes in hot spots and resultant changes in the SERS activity.^{30d} To evaluate the SERS activity of the GNR assemblies at various stages of assembly, SERS spectra were measured from samples, at various stages of the assembly. The prominent Raman bands in the SERS spectrum of CV are summarized in Supporting Information Figure S13.^{30e} Initially, GNRs did not show any appreciable SERS activity (Figure 7B, spectrum a), but the assembled structures induced by EDTA showed excellent SERS activity. Most intense peaks of CV can be seen in spectra b and c (Figure 7B).^{30e} In the case of end-to-end assembled gold nanorod chains (spectrum b, EDTA concentration of 0.15 mM), all prominent peaks due to CV can be seen. The ‘hot spots’ formed between the two tips of GNRs might be the primary reason for this SERS activity. As the concentration of EDTA increased to 0.75 mM, sheet-like assembled structures are formed, and this structure is much more Raman enhancing (Figure 7B, spectrum c) than that of the end-to-end assembled rods primarily due to the presence of more hot spots created by the presence of more rods. This was illustrated in the SERS spectrum of CV as well. In addition to the prominent features present in the case of spectrum b, additional low intensity features also emerged in the case of these structures. We can see in the spectrum (Figure 7B, spectrum c) the features centered at 1490, 1460, 1135, 995, 780, 754, 641, 590, 545, 368, 246 cm^{-1} , some of which were absent in ‘b’, implying the higher SERS activity of sheet-like superstructures.^{30e} After the addition of metal ion (Pb^{2+} , 200 ppm), the assembled structures become disassembled. After disassembly, the structure did not show much Raman enhancement (Figure 7B, spectrum d), but compared to parent nanorods, some signals of CV were seen in the spectrum. This is probably due to the small assembled structures present even after the disassembling process. Hence, depending upon the form of assembly, the SERS enhancement varied and we were able to tune the SERS activity of the assembly by controlling the concentration of EDTA added or by adding metal ion into the already assembled structure.

CTAB present on the GNRs are not expected to hinder the SERS activity of GNRs.^{30f} The Raman spectra of parent gold nanorod did not show any prominent Raman features of the CTAB molecule (Supporting Information Figure S14). In the

centrifuged sample, the amount of CTAB will be minimal compared to the as-prepared sample. Hence, the interaction between CV and GNRs should be feasible. The SERS activity is highly dependent on the morphology of nanostructures as well. In order to prove the high SERS activity of assembled gold nanorods, a comparative study was carried out. We measured the SERS spectrum of CV molecules from spherical nanoparticles prepared by the Turkovich method³¹ and gold nanorod assembly (Supporting Information Figure S15). A considerable increase in the Raman intensity was observed in the case of gold nanorod assembly, which could be attributed to the large electric field enhancement experienced by the analyte sitting in-between the tips of two nanorods. This result suggests that the assembled gold nanorods are superior in view of SERS activity compared to other substrates such as spherical nanoparticles, Au films, etc. Aggregates of nanoparticles are known to show good SERS activity due to the formation of a large number of hot spots,^{30f} but sensitivity and reproducibility are major concerns in such measurements. In the case of periodically arranged nanosubstrates, much better and reproducible SERS intensity can be expected. Compared to aggregates of spherical nanoparticles, GNR assembly showed enhanced SERS activity (Supporting Information Figure S15). This might be due to the large electromagnetic enhancement at the tip of the nanorod.^{30g} The repeated use of the aggregated structures resulted in a varying extent of SERS activity, but the assembled system showed almost constant SERS activity (Supporting Information Figure S16). This proves the superiority of assembled superstructures over aggregated nanostructures.

Reversibility of Assembly–Disassembly Process. The reversibility of the assembly process was checked. After disassembly (GNR_{AD}), EDTA (0.75 mM) was added again to the sample to check the reversibility of the assembly. The addition of EDTA produced observable changes in the UV/vis spectra. The addition of EDTA to GNR_{AD} resulted in an increase in background and a concurrent broadening of the LSP. The LSP showed a blue shift as well. However, these changes were smaller compared to those of the parent nanorods (dotted line in Figure 8A). However, the addition of $\text{Pb}(\text{II})$ to the mixture again shifted the LSP to the initial position, indicating disassembly. The changes in the assembly process may be attributed to the dilution effect. The addition of EDTA and metal ions have changed the concentration of NRs in the suspension and hence bring these NRs to well-arranged superstructures previously unfeasible. Still, small assemblies formed as indicated by the broadening and shift in the LSP as well as the rise in the background. The proposal was cross-checked by centrifuging the GNR_{AD} to remove the unwanted material and redispersing it to the optimum initial concentration. First, GNR_{AD} was centrifuged at 4000 rpm to remove the assembled structures. The supernatant was again centrifuged at 11000 rpm, and the residue was redispersed to an optimum optical density of 2.5. This corresponds to free NRs, which is designated as GNR_{Cen} . The spectral changes of GNR_{Cen} upon addition of EDTA and its comparison to the spectrum of parent GNR are given in Figure 8B. We can see that the UV/vis spectrum of GNR_{Cen} is very similar to the spectra of initial GNRs. The spectral changes accompanying the addition of EDTA are also similar. The system can be disassembled similar to that accomplished with parent GNRs. The process was found to be reversible three times, and afterward, nanorods became settled due to irreversible aggregation. Repeated centrifugation–redispersion cycles progressively remove CTAB from the GNR surface, and in the absence of stabilizing agent, GNRs undergo aggregation-induced settling. In order to increase the reversibility, CTAB can be exchanged with some other molecules.

Thiols and cationic phospholipids are the two major species that were tested to replace CTAB on gold nanorods.²³ Thiols can lead to the assembly. Even after exchange, repeated centrifugation can result in aggregation here as well. Moreover, the present methodology of assembly and disassembly works through an electrostatic mechanism. Hence, the possible replacements of CTAB are limited. Therefore, the possible alternative is cationic phospholipids.²³ This will enhance the biocompatibility. However, the interaction of gold with CTAB and phospholipids is similar, so the stability against centrifugation is expected to be limited. Therefore, this direction of study was not pursued.

CONCLUSIONS

A facile method for the reversible assembly and disassembly of gold nanorods induced by EDTA was investigated. The nature of the assembly can be changed from end-to-end (leading to chains) to side-by-side (leading to sheets) by controlling the EDTA concentration. The former type of assembly occurred at lower concentrations of EDTA (0.15 mM). When the concentration of EDTA was increased, these chains came together and formed sheets by side-by-side assembly. The assemblies can be destabilized in the presence of metal ions by EDTA, which is a good chelating agent. Due to the higher affinity of EDTA to metal ions, they detach from the GNRs to form more stable metal ion complexes, resulting in the disassembly of the GNR superstructures. The disassembly process was studied in detail, taking Pb(II) as the model metal ion. The disassembly proceeded in the following order: side-by-side-sheets to bundled chains to single end-to-end chains to dispersed individual GNRs. At lower concentrations of Pb(II), bundled chains formed. The UV/vis data support these observations. As the concentration of metal ion increased gradually, the LSP showed a concurrent decrease in intensity as well as a blue shift. TEM investigations revealed the existence of bundled chains at this concentration range. At a concentration of 500 ppb of metal ions, individual bundled chains were seen. At a concentration of 25 ppm Pb(II), the higher wavelength absorption became prominent and TEM showed end-to-end arranged structures. When the concentration reached 300 ppm, the peak position almost coincided with the LSP of the parent GNR, showing complete disassembly. The SERS activity of the assembled structures was also investigated. Reversibility of the system was investigated, and we found that the system is reversible up to three times after which GNRs undergo irreversible aggregation due to the unavailability of the stabilizing agent.

ASSOCIATED CONTENT

S Supporting Information. TEM images: end-to-end assembled rods where EDTA is proposed to be attached to GNR tips, small islands of GNRs formed at 0.2 mM EDTA, small assembled structures after disassembly, ladder-like assemblies formed at pH = 3.5, randomly arranged rods upon the addition of a EDTA–Pb(II) complex, and the disassembly with Fe(II) and Fe(III); UV/vis spectra: the spectral changes of side-by-side assembled GNRs for some ions tested, detection of Pb²⁺ in ppb range, and the disassembly with Fe(II) and Fe(III); FT-IR spectra of the assembly and disassembly. A table depicting Raman features of CV. This material is available free of charge via the Internet at <http://pubs.acs.org>.

AUTHOR INFORMATION

Corresponding Author

*E-mail: pradeep@iitm.ac.in. Tel: 91-44-2257-4208.

ACKNOWLEDGMENT

We thank the Nanoscience and Nanotechnology Initiative of DST, Government of India, for supporting our research program.

REFERENCES

- (1) (a) Yu, Y. Y.; Chang, S. S.; Lee, C. L.; Wang, C. R. C. *J. Phys. Chem. B* **1997**, *101*, 6661. (b) Van der Zande, B. M. I.; Bohmer, M. R.; Fokkink, L. G. J.; Schonenberger, C. *J. Phys. Chem. B* **1997**, *101*, 852. (c) Link, S.; Mohamed, M. B.; El-Sayed, M. A. *J. Phys. Chem. B* **1999**, *103*, 3073. (d) Sau, T. K.; Murphy, C. J. *Langmuir* **2004**, *20*, 6414. (e) Pérez-Juste, J.; Pastoriza-Santos, I.; Liz-Marzán, L. M.; Mulvaney, P. *Coord. Chem. Rev.* **2005**, *249*, 1870.
- (2) (a) Tsung, C. K.; Kou, X.; Shi, Q.; Zhang, J.; Yeung, M. H.; Wang, J.; Stucky, G. D. *J. Am. Chem. Soc.* **2006**, *128*, 5352. (b) Sreeprasad, T. S.; Samal, A. K.; Pradeep, T. *Langmuir* **2007**, *23*, 9463.
- (3) (a) Adams, M.; Dogic, Z.; Keller, S. L.; Fraden, S. *Nature* **1998**, *393*, 349. (b) Whitesides, G. M.; Boncheva, M. *Proc. Natl. Acad. Sci. U.S.A.* **2002**, *99*, 4769.
- (4) (a) Nikoobakht, B.; Wang, Z. L.; El-Sayed, M. A. *J. Phys. Chem. B* **2000**, *104*, 8635. (b) Sau, T. K.; Murphy, C. J. *Langmuir* **2005**, *21*, 2923. (c) Guerrero-Martínez, A.; Pérez-Juste, J.; Carbó-Argibay, E.; Tardajos, G.; Liz-Marzán, L. M. *Angew. Chem., Int. Ed.* **2009**, *48*, 9484.
- (5) (a) Korgel, B. A.; Zaccheroni, N.; Fitzmaurice, D. *J. Am. Chem. Soc.* **1999**, *121*, 3533. (b) Murray, C. B.; Kagan, C. R.; Bawendi, M. G. *Science* **1995**, *270*, 1335. (c) Talapin, D. V.; Shevchenko, E. V.; Kornowski, A.; Gaponik, N.; Haase, S.; Rogach, A. L.; Weller, H. *Adv. Mater.* **2001**, *13*, 1868. (d) Sun, S.; Murray, C. B.; Weller, D.; Folks, L.; Moser, A. *Science* **2000**, *287*, 1989. (e) Lin, Y.; Skaff, H.; Emrick, T.; Dinsmore, A. D.; Russell, T. P. *Science* **2003**, *299*, 226. (f) Cox, J. K.; Eisenberg, A.; Lennox, R. B. *Curr. Opin. Colloid Interface Sci.* **1999**, *4*, 52. (g) Lopes, W. A.; Jaeger, H. M. *Nature* **2001**, *414*, 735.
- (6) (a) Jain, P. K.; Eustis, S.; El-Sayed, M. A. *J. Phys. Chem. B* **2006**, *110*, 18243. (b) Draine, B. T.; Goodman, J. *Astrophys. J.* **1993**, *405*, 685.
- (7) (a) Zhang, S.; Kou, X.; Yang, Z.; Shi, Q.; Stucky, G. D.; Sun, L.; Wang, J.; Yan, C. *Chem. Commun.* **2007**, 1816. (b) Sreeprasad, T. S.; Samal, A. K.; Pradeep, T. *Langmuir* **2008**, *24*, 4589. (c) Orendorff, C. J.; Hankins, P. L.; Murphy, C. J. *Langmuir* **2005**, *21*, 2022.
- (8) Ni, W.; Mosquera, R. A.; Pérez-Juste, J.; Liz-Marzán, L. M. *J. Phys. Chem. Lett.* **2010**, *1*, 1181.
- (9) Joseph, S. T. S.; Ipe, B. I.; Pramod, P.; Thomas, K. G. *J. Phys. Chem. B* **2005**, *110*, 150.
- (10) (a) Mitamura, K.; Imae, T.; Saito, N.; Takai, O. *J. Phys. Chem. B* **2007**, *111*, 8891. (b) Nakashima, H.; Furukawa, K.; Kashimura, Y.; Torimitsu, K. *Langmuir* **2008**, *24*, 5654.
- (11) (a) Dujardin, E.; Hsin, L. B.; Wang, C. R. C.; Mann, S. *Chem. Commun.* **2001**, 1264. (b) Pan, B.; Ao, L.; Gao, F.; Tian, H.; He, R.; Cui, D. *Nanotechnology* **2005**, 1776. (c) Wang, C.; Chen, Y.; Wang, T.; Ma, Z.; Su, Z. *Chem. Mater.* **2007**, *19*, 5809. (d) Caswell, K. K.; Wilson, J. N.; Bunz, U. H. F.; Murphy, C. J. *J. Am. Chem. Soc.* **2003**, *125*, 13914. (e) Wang, Y.; Li, Y. F.; Wang, J.; Sanga, Y.; Huang, C. Z. *Chem. Commun* **2010**, *46*, 1332.
- (12) (a) Correa-Duarte, M. A.; Pérez-Juste, J.; Sanchez-Iglesias, A.; Giersig, M.; Liz-Marzán, L. M. *Angew. Chem., Int. Ed.* **2005**, *44*, 4375. (b) Khanal, B. P.; Zubarev, E. R. *Angew. Chem., Int. Ed.* **2007**, *46*, 2195. (c) Kumar, V. R. R.; Samal, A. K.; Sreeprasad, T. S.; Pradeep, T. *Langmuir* **2007**, *23*, 8667. (d) Wang, C.; Chen, Y.; Wang, T.; Ma, Z.; Su, Z. *Adv. Funct. Mater.* **2008**, *18*, 355. (e) Das, M.; Mordoukhovski, L.; Kumacheva, E. *Adv. Mater.* **2008**, *20*, 2371.
- (13) Nie, Z.; Fava, D.; Rubinstein, M.; Kumacheva, E. *J. Am. Chem. Soc.* **2008**, *130*, 3683.

- (14) (a) Hazarika, P.; Ceyhan, B.; Niemeyer, C. M. *Angew. Chem., Int. Ed.* **2004**, *43*, 6469. (b) Sharma, J.; Chhabra, R.; Yan, H.; Liu, Y. *Chem. Commun* **2007**, 477.
- (15) (a) Sun, Z.; Ni, W.; Yang, Z.; Kou, X.; Li, L.; Wang, J. *Small* **2008**, *4*, 1287. (b) Chan, Y.-T.; Li, S.; Moorefield, C. N.; Wang, P.; Shreiner, C. D.; Newkome, G. R. *Chem.—Eur. J.* **2010**, *16*, 4164.
- (16) (a) Wang, Z. L.; Gao, R. P.; Nikoobakht, B.; El-Sayed, M. A. *J. Phys. Chem. B* **2000**, *104*, 5417. (b) Carbó-Argibay, E.; Rodríguez-González, B.; Gómez-Graña, S.; Guerrero-Martínez, A.; Pastoriza-Santos, I.; Pérez-Juste, J.; Liz-Marzán, L. M. *Angew. Chem., Int. Ed.* **2010**, *49*, 9397.
- (17) Kawamura, G.; Yang, Y.; Nogami, M. *J. Phys. Chem. C* **2008**, *112*, 10632.
- (18) Pérez, M. R.; Pavlovic, I.; Barriga, C.; Cornejo, J.; Hermosín, M. C.; Ulibarri, M. A. *Appl. Clay Sci.* **2006**, *32*, 245.
- (19) Allara, D. L.; Atre, S. V.; Elliger, C. A.; Snyder, R. G. *J. Am. Chem. Soc.* **1991**, *113*, 1852.
- (20) (a) Orthgiess, E.; Dobias, B. *Colloid Surface A* **1994**, *83*, 129. (b) Huo, Q.; Margolese, D. I.; Ciesla, U.; Demuth, D. G.; Feng, P.; Gier, T. E.; Sieger, P.; Firouzi, A.; Chmelka, B. F.; Schuth, F.; Stucky, G. D. *Chem. Mater.* **1994**, *6*, 1176.
- (21) Vial, S.; Pastoriza-Santos, I.; Pérez-Juste, J.; Liz-Marzán, L. M. *Langmuir* **2007**, *23*, 4606.
- (22) Chapman, D.; Lloyd, D. R.; Prince, R. H. *J. Chem. Soc.* **1963**, 3645.
- (23) Orendorff, C. J.; Alam, T. M.; Sasaki, D. Y.; Bunker, B. C.; Voigt, J. A. *ACS Nano* **2009**, *3*, 971.
- (24) Sawyer, D. T.; Paulsen, P. J. *J. Am. Chem. Soc.* **1959**, *81*, 816.
- (25) Höbel, B.; Sonntag, C. V. *J. Chem. Soc., Perkin Trans.* **1998**, *2*, 509.
- (26) (a) Gole, A.; Orendorff, C. J.; Murphy, C. J. *Langmuir* **2004**, *20*, 7117. (b) Boca, S. C.; Astilean, S. *Nanotechnology* **2010**, *21*, 235601.
- (27) (a) Moskovits, M. *Rev. Mod. Phys.* **1985**, *57*, 783. (b) Chang, R. K.; Furtak, T. E. *Surface Enhanced Raman Scattering*; Plenum Press: New York, 1982.
- (28) (a) Campion, A.; Kambhampati, P. *Chem. Soc. Rev.* **1998**, *27*, 241. (b) Jeong, D. H.; Zhang, Y. X.; Moskovits, M. *J. Phys. Chem. B* **2004**, *108*, 12724. (c) Tao, A.; Kim, F.; Hess, C.; Goldberger, J.; He, R.; Sun, Y.; Xia, Y.; Yang, P. *Nano Lett.* **2003**, *3*, 1229.
- (29) (a) Orendorff, C. J.; Gearheart, L.; Jana, N. R.; Murphy, C. J. *Phys. Chem. Chem. Phys.* **2006**, *8*, 165. (b) Hu, X.; Cheng, W.; Wang, T.; Wang, Y.; Wang, E.; Dong, S. *J. Phys. Chem. B* **2005**, *109*, 19385. (c) Huang, X.; El-Sayed, I. H.; Qian, W.; El-Sayed, M. A. *Nano Lett.* **2007**, *7*, 1591. (d) Yun, S.; Oh, M. K.; Kim, S. K.; Park, S. *J. Phys. Chem. C* **2009**, *113*, 13551.
- (30) (a) Lee, S. J.; Morrill, A. R.; Moskovits, M. *J. Am. Chem. Soc.* **2006**, *128*, 2200. (b) Gunnarsson, L.; Rindzevicius, T.; Prikulis, J.; Kasemo, B.; Kall, M.; Zou, S. L.; Schatz, G. C. *J. Phys. Chem. B* **2005**, *109*, 1079. (c) Schuck, P. J.; Fromm, D. P.; Sundaramurthy, A.; Kino, G. S.; Moerner, W. E. *Phys. Rev. Lett.* **2005**, *94*, 017402. (d) Chen, T.; Wang, H.; Chen, G.; Wang, Y.; Feng, Y.; Teo, W. S.; Wu, T.; Chen, H. *ACS Nano* **2010**, *4*, 3087. (e) Shibu, E. S.; Kimura, K.; Pradeep, T. *Chem. Mater.* **2009**, *21*, 3773. (f) Sudipto, P.; Depero, L. E.; Alessandri, I. *Nanotechnology* **2010**, *21*, 425701. (g) Li, J. F.; Huang, Y. F.; Ding, Y.; Yang, Z. L.; Li, S. B.; Zhou, X. S.; Fan, F. R.; Zhang, W.; Zhou, Z. Y.; WuDe, Y.; Ren, B.; Wang, Z. L.; Tian, Z. Q. *Nature* **2010**, *464*, 392.
- (31) Turkevich, J.; Stevenson, P. C.; Hillier, J. *Discuss. Faraday Soc.* **1951**, *11*, 55.